

# ReverbMiipher: Generative Speech Restoration meets Reverberation Characteristics Controllability

Wataru Nakata<sup>1,2\*</sup>, Yuma Koizumi<sup>1</sup>, Shigeki Karita<sup>1</sup>, Robin Scheibler<sup>1</sup>, Haruko Ishikawa<sup>1</sup>, Adriana Guevara-Rukoz<sup>3</sup>, Heiga Zen<sup>1</sup>, Michiel Bacchiani<sup>1</sup>

<sup>1</sup> Google DeepMind, Tokyo, Japan <sup>2</sup>The University of Tokyo, Tokyo, Japan <sup>3</sup>Google, Zurich, Switzerland  
wnakata@google.com, koizumiyuma@google.com

**Abstract**—Reverberation encodes spatial information regarding the acoustic source environment, yet traditional Speech Restoration (SR) usually completely removes reverberation. We propose *ReverbMiipher*, an SR model extending parametric resynthesis framework, designed to denoise speech while preserving and enabling control over reverberation. *ReverbMiipher* incorporates a dedicated ReverbEncoder to extract a reverb feature vector from noisy input. This feature conditions a vocoder to reconstruct the speech signal, removing noise while retaining the original reverberation characteristics. A stochastic zero-vector replacement strategy during training ensures the feature specifically encodes reverberation, disentangling it from other speech attributes. This learned representation facilitates reverberation control via techniques such as interpolation between features, replacement with features from other utterances, or sampling from a latent space. Objective and subjective evaluations confirm *ReverbMiipher* effectively preserves reverberation, removes other artifacts, and outperforms the conventional two-stage SR and convolving simulated room impulse response approach. We further demonstrate its ability to generate novel reverberation effects through feature manipulation.

## 1. INTRODUCTION

Reverberation, a phenomenon originating from the complex interplay of sound reflections and diffractions within an enclosed space [1], encodes spatial information regarding the acoustic source environment that is fundamental to spatial perception [2], [3]. Consequently, the accurate rendering of reverberation is critical for enhancing the immersive quality of technologies such as Augmented Reality and Virtual Reality [2], [4].

As generative models continue to demonstrate expanding capabilities in creating diverse media content [5], [6], the need for speech processing methods that can preserve and control the spatial properties encoded in reverberation is becoming increasingly important. Historically, however, speech denoising research has primarily focused on removing reverberation, often treating it as undesirable noise that negatively impacts speech intelligibility [7]–[12]. Recent advancements show that modern speech restoration (SR) techniques are capable of transforming noisy, reverberant recordings into high-fidelity, studio-quality audio [13]–[26]. Considering the success of generative models in various speech generation tasks [6], it is logical to pursue generative speech restoration models capable not only of cleaning audio but also of actively preserving and controlling reverberation characteristics. Such models would offer creation of realistic and diverse datasets for audio spatial understanding models. Furthermore, they would enable dynamic reverberation preservation or manipulation, offering fine-grained control over the acoustical environment in recent video generation models [27], [28].

Regarding reverberation control, room acoustics simulation has remained a field of active research since the 1960s, spawning a wide array of geometric [29], [30], wave-based [31], and deep learning techniques [32]–[34]. One potential approach for our task involves deriving a dry source signal using SR, followed by a

convolution with a simulated room impulse response (RIR). However, this two-stage process faces limitations, notably the difficulty of explicit RIR estimation, and the susceptibility to error propagation, potentially compromising output audio fidelity. Consequently, end-to-end architectures that directly manage reverberation offer a potentially more robust alternative, drawing parallels with successful fully neural [35], [36] or language model-based [6] systems used in fields like speech synthesis and conversion.

We propose *ReverbMiipher*, an SR model based on Miipher-2 [26], designed to preserve and manipulate reverberation while removing noise. Extending Miipher-2’s parametric resynthesis approach, *ReverbMiipher* incorporates a ReverbEncoder network that extracts a dedicated reverb-feature vector encoding reverberation information from the noisy input. Conditioning a vocoder with this feature yields a denoised waveform that preserves the original reverberation. To ensure this feature captures only reverberation, training involves stochastically replacing it with a zero-vector, directing the model to output the anechoic source waveform under this condition. This architecture enables reverberation control by manipulating the reverb feature, e.g., via replacement using features from other utterances, interpolation, or sampling from a learned latent space. Objective and subjective evaluations demonstrate that *ReverbMiipher* removes artifacts while preserving reverberation, outperforming the two-stage approach, i.e. SR output convolved with simulated RIRs. We also demonstrate generation of novel reverberation via interpolation or principal component analysis (PCA)-based latent space sampling of the model’s reverb features. Speech samples are available online<sup>1</sup>.

## 2. CONVENTIONAL METHODS

### 2.1. Generative speech restoration

In this paper, SR is defined as the task of estimating a high-quality signal by removing all forms of speech degradation, including but not limited to enhancement [37], dereverberation [7]–[12], declipping [38], and super-resolution [39], [40]. This task is also referred to in other literature as “Universal Speech Enhancement” [41] or “High-Fidelity Speech Enhancement” [23]. Let the  $T$ -sample time-domain signal  $\mathbf{x} \in \mathbb{R}^T$  be a degraded observation of an original signal  $\mathbf{s} \in \mathbb{R}^T$ . The goal of SR is to find a function  $\mathcal{F}$  that estimates  $\mathbf{s}$  from  $\mathbf{x}$  as  $\mathbf{y} = \mathcal{F}(\mathbf{x}) \in \mathbb{R}^T$ .

Current trends in SR research indicate a shift from paradigms based on the modification of  $\mathbf{x}$ , such as time-frequency masking [37], to those focused on the direct synthesis of  $\mathbf{s}$  utilizing generative models [13]–[26]. Generative model-based approaches estimate the probability distribution of  $\mathbf{s}$  conditioned on  $\mathbf{x}$ . The output signal is then obtained by sampling from this estimated distribution, i.e.  $\mathbf{y} \sim p(\mathbf{s} | \mathbf{x})$ . A potential consequence of this waveform generation process is the divergence of speech content or speaker characteristics

\*Work done during internship at Google

<sup>1</sup>[https://google.github.io/df-conformer/reverb\\_miipher/](https://google.github.io/df-conformer/reverb_miipher/)

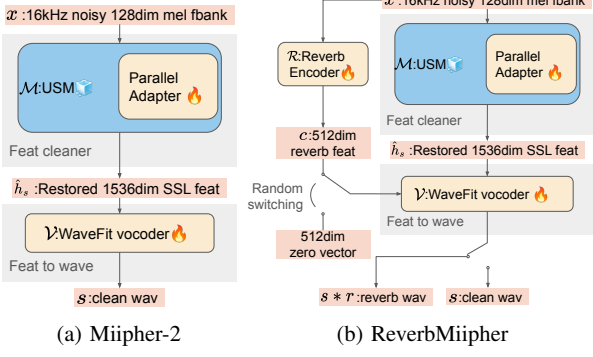


Fig. 1: Overview of (a) Miipher-2 and (b) the proposed ReverbMiipher.

in  $\mathbf{y}$  from those of  $\mathbf{s}$ . To mitigate this, state-of-the-art techniques incorporate conditioning inputs (e.g., on text, speaker ID), employ loss functions to maintain phonemic consistency [21], [24], or leverage self-supervised learning (SSL) models for robust feature extraction [18].

## 2.2. Miipher-2

Miipher-2 [26] is a generative SR model based on a parametric resynthesis strategy [13]. An overview of Miipher-2 is shown in Fig. 1a, which comprises two primary components: a feature cleaner, which predicts acoustic features corresponding to a clean waveform from an input noisy waveform, and a vocoder, which subsequently synthesizes a waveform from these predicted clean features.

First, the feature cleaner predicts an SSL feature corresponding to clean speech signal  $\mathbf{h}_s = \mathcal{M}(\mathbf{s})$  from a given 128 mel-bands log-mel spectrogram of  $\mathbf{x}$ . Miipher-2 uses pre-trained Universal Speech Model (USM) [42] as  $\mathcal{M}$ . To predict  $\mathbf{h}_s$  from  $\mathbf{x}$ , Miipher-2 connects parallel adapters [43] to each Conformer [44] layer in USM as  $\mathcal{M}_a$ , i.e.  $\hat{\mathbf{h}}_s = \mathcal{M}_a(\mathbf{x})$ . During training only the parallel adapter layers are updated. The loss function is a sum of mean squared error, mean absolute error and a spectral convergence loss which can be expressed as  $\mathcal{L}_{\mathcal{M}_a} = \|\mathbf{h}_s - \hat{\mathbf{h}}_s\|_1 + \|\mathbf{h}_s - \hat{\mathbf{h}}_s\|_2^2 + \|\mathbf{h}_s - \hat{\mathbf{h}}_s\|_2^2 / \|\mathbf{h}_s\|_2^2$ .

Then, the neural vocoder converts  $\hat{\mathbf{h}}_s$  to  $\mathbf{y} = \mathcal{V}(\hat{\mathbf{h}}_s)$ . As the neural vocoder, Miipher-2 uses WaveFit [45] which is inspired by diffusion models and fixed-point iteration. It transforms random numbers into a waveform conditioned on input features, therefore, by conditioning it by  $\hat{\mathbf{h}}_s$  this process can be regarded as sampling from  $p(\mathbf{s} | \mathbf{x})$ . First,  $\mathcal{V}$  is pre-trained by using ground truth SSL features to minimize  $\mathcal{L}_{\mathcal{V}}(\mathbf{s}, \mathcal{V}(\mathbf{h}_s))$  where  $\mathcal{L}_{\mathcal{V}}$  is the loss function of WaveFit. Then,  $\mathcal{V}$  is finetuned using the predicted SSL feature to minimize  $\mathcal{L}_{\mathcal{V}}(\mathbf{s}, \mathcal{V}(\hat{\mathbf{h}}_s))$ . For the details of the implementation, please refer to [26].

## 3. REVERBMIIPHER

### 3.1. Model overview

The proposed method, ReverbMiipher, is an extended model of Miipher-2 endowed with reverberation controllability as shown in Fig. 1b. This model incorporates an additional feature extraction module termed ReverbEncoder  $\mathcal{R}$ . The ReverbEncoder takes a log-mel spectrogram extracted from  $\mathbf{x}$  and outputs a reverb-feature  $\mathbf{c} = \mathcal{R}(\mathbf{x}) \in \mathbb{R}^D$ , which is a vector embedded with reverberation characteristics. Here,  $D = 512$  is the dimension of the reverb-feature. By using  $\mathbf{c}$  as an additional conditioning for  $\mathcal{V}$ , ReverbMiipher outputs a signal in which only reverberation is preserved and all other artifacts are removed as  $\mathcal{V}(\hat{\mathbf{h}}_s, \mathbf{c})$ . Furthermore, applying control to  $\mathbf{c}$  enables the manipulation of reverberation.

### 3.2. ReverbEncoder training

ReverbEncoder  $\mathcal{R}$  consists of a stack of four Conformer [44] layers with a kernel size of five in the convolution module, followed by mean pooling along the time axis. The input of  $\mathcal{R}$  is a 128-dimensional log-mel filterbank, which is also used by  $\mathcal{M}_a$ .

A challenge in training the ReverbEncoder is to disentangle reverberation from other acoustic information. If this disentanglement is not achieved, manipulating or interpolating  $\mathbf{c}$  to control the reverberation of the output signal will also alter information such as speaker identity and speech content. To address this, a stochastic switching technique was introduced during the training of both  $\mathcal{R}$  and  $\mathcal{V}$ . In the creation of supervised training data, the input waveform  $\mathbf{x}$  was generated from the clean speech signal  $\mathbf{s}$  according to  $\mathbf{x} = \mathcal{A}(\mathbf{s} * \mathbf{r} + \mathbf{n})$ , where  $*$  is convolution,  $\mathbf{r}$  is an RIR,  $\mathbf{n} \in \mathbb{R}^T$  is a noise waveform, and  $\mathcal{A}$  signifies a sequence of additional artifact operators, such as codec artifacts and band-width filters. This switching between the reverberant target and the clean speech target is performed independently for each sample within a mini-batch. Consequently, a mini-batch comprises samples targeting both clean and reverberant speech.  $\mathcal{R}$  and  $\mathcal{V}$  are then trained by minimizing the loss function:

$$\mathcal{L}_{\mathcal{R}} = \begin{cases} \mathcal{L}_{\mathcal{V}}(\mathbf{s} * \mathbf{r}, \mathcal{V}(\hat{\mathbf{h}}_s, \mathbf{c})) & \text{if } \mathcal{U}(0, 1) > q \\ \mathcal{L}_{\mathcal{V}}(\mathbf{s}, \mathcal{V}(\hat{\mathbf{h}}_s, \mathbf{0})) & \text{otherwise} \end{cases}, \quad (1)$$

where  $\mathcal{U}(0, 1)$  is a uniform random number with values between 0 and 1,  $\mathbf{0}$  is a  $D$ -dimensional zero-vector, and the hyperparameter  $q = 0.1$  is the switching probability of the loss function.

The feature cleaner  $\mathcal{M}_a$  is trained using the Miipher-2's (Section 2.2) methodology. This training approach assumes that the estimated clean speech features  $\hat{\mathbf{h}}_s$  exclusively contain speech information, devoid of reverberation, noise, or other artifacts. By defining the model's output as  $\mathbf{s}$  when the reverberation conditioning vector is  $\mathbf{0}$ , the model is explicitly trained to interpret a zero-vector as the absence of reverberation, enabling speech reconstruction solely from  $\hat{\mathbf{h}}_s$ . Furthermore, given the target signal is  $\mathbf{s} * \mathbf{r}$  when the reverberation feature is input to the network, any artifacts present in  $\mathbf{c}$  other than reverberation will be treated as noise by the network. Consequently, the ReverbEncoder weights are expected to be updated to selectively preserve information pertaining only to reverberation.

## 4. EXPERIMENTS

We demonstrate the efficacy of the proposed method in: (i) preserving reverberation from noisy signals while simultaneously removing other noise and artifacts; and (ii) enabling the manipulation of reverberation through the reverb-feature. The former claim (i) is substantiated in this section through a comparative evaluation of the proposed method with conventional techniques, employing both objective and subjective assessments. The latter claim (ii) is exemplified via case studies in the sections that follow.

### 4.1. Comparison method

To our knowledge, the task of reverberation-controllable SR has not been extensively investigated in prior research. For instance, speech enhancement models primarily designed for denoising may preserve reverberation in the output signal but are often incapable of mitigating other distortions, such as codec artifacts. While generative SR models can be trained with reverberant speech as the target, this approach lacks explicit control over the reverberation characteristics. Therefore, this paper introduces a baseline system consisting of a conventionally trained SR model, the output of which is subsequently convolved with a synthesized RIR. The Miipher-2 model is utilized as the SR

component, given its foundational role in the proposed architecture. This baseline system is henceforth designated as **Miipher-RIR**.

The two-stage processing pipeline of Miipher-RIR requires the estimation of both the anechoic signal and the RIR from the noisy input. However, estimating the RIR from a noisy signal presents an inherently challenging problem. Therefore, in this study, the RIR is simulated using the image method [29], under the assumption that reverberation time (RT60) and direct-to-reverberant ratio (DRR) are perfectly known. It should be noted that, as practical estimation of these parameters typically incurs errors, the Miipher-RIR performance metrics reported herein likely represent an upper bound compared to those achievable in real-world scenarios.

Initially, RT60 and DRR values were computed from the ground-truth RIR. Subsequently, twenty RIRs were simulated using the image method implemented in pyroomacoustics simulator [46], employing the ground-truth RT60 and randomly assigning source and microphone positions within the simulated enclosure. From these simulations, the RIR exhibiting the DRR value closest to the target was selected for convolution with the output of the Miipher-2 model. The DRR was calculated from the RIR according to the definition provided in [47], assuming a direct sound segment length of 8 ms.

#### 4.2. Experimental conditions

**Training dataset:** Training was performed using the FLEURS-R speech corpus [48]. FLEURS-R is a large-scale multilingual corpus containing approximately 1,300 hours of speech across 102 languages at a sampling rate of 24kHz. Noisy training samples were created by mixing clean speech from FLEURS-R with noise from the internal dataset at random Signal-to-Noise Ratios (SNRs) ranging from 5 dB to 30 dB. Data augmentation techniques included applying reverberation (using the simulated RIRs by the image method) and simulating various codec artifacts including MP3, Vorbis, A-law, AMR-WB, and OPUS codecs following previous work [18], [26].

**Evaluation dataset:** Evaluation was conducted on a simulated test set created using real recorded RIRs and noise sources distinct from the training data. The clean speech source for the evaluation set was the EARS dataset [49]. Ten random utterances were selected per speaker. The number of total utterances was 1070. The noise sources for the evaluation set were taken from the WHAM! dataset [50]. Real-world RIRs were sourced from the MIT Acoustical Reverberation Scene Statistics Survey [51]. Test samples were generated by first convolving the clean speech with an RIR from the MIT survey, then adding WHAM! noise at random SNR ranging from -5 dB to 20 dB. Finally, a codec simulation was applied, randomly selecting from MP3, Vorbis, A-law, AMR-WB, and OPUS for each sample.

**Optimizer:** We used an Adam [52] with  $\beta_1 = 0.9, \beta_2 = 0.98$  for the vocoder, and  $\beta_1 = 0.9, \beta_2 = 0.999$  for the feature cleaner. Learning rate warmup was applied for 5000 steps. The number of training steps were 2 million steps for ReverbEncoder and vocoder, and 250k steps for feature cleaner. The batch size was 512.

#### 4.3. Subjective evaluation

A subjective evaluation was conducted to assess the perceptual similarity of reverberation. Given that evaluating subtle reverberation changes can be challenging and may require audio expertise, a standard Mean Opinion Score test, which commonly solicit overall quality judgments, was deemed unsuitable for crowdsourced human reviewers who might lack this specific expertise. Therefore, a pairwise comparison method with ranking was employed. This approach directs listeners' focus, regardless of expertise, specifically onto reverberant characteristics through direct comparison. Human reviewers first

Table 1: Subjective evaluation results. **Bold** font shows the best results.  $p$ -values are calculated using pairwise Wilcoxon test [53] with Bonferroni correction [54].

Model	Mean rank $\downarrow$	$p$ -value	
		Miipher-RIR	ReverbMiipher
Miipher-2	2.50	$< 10^{-8}$	$< 10^{-8}$
Miipher-RIR	2.01	-	$< 10^{-8}$
ReverbMiipher	<b>1.49</b>	-	-

Table 2: Objective evaluation results. **Bold** font shows the best results among the restored speech.

Model	MCD ( $\downarrow$ )	GPE ( $\downarrow$ )	SPK-sim ( $\uparrow$ )
Noisy input	8.52	0.09	0.79
Miipher-2	7.28	0.16	0.63
Miipher-RIR	6.76	0.19	0.71
ReverbMiipher (ours)	<b>5.26</b>	<b>0.16</b>	<b>0.79</b>

listened to the ground truth reverberant speech, then ranked corresponding samples from Miipher-2, Miipher-RIR, and ReverbMiipher based on reverberation similarity to the ground truth. The presentation order of these 3 samples were randomized. The evaluation involved 557 reviewers, each evaluating a maximum of 7 sample sets, yielding 2,878 total ratings. All human reviewers were required to use headphones. Table 1 details the results of the subjective evaluation. The proposed ReverbMiipher yielded reverberation most similar to the ground truth, relative to the other models with statistical significance. Therefore, ReverbMiipher successfully preserves perceptually similar reverberation in SR.

#### 4.4. Objective evaluation

Performance was assessed using objective metrics calculated by comparing the model outputs against the ground truth reverberant speech (i.e.  $s * r$ ). The metrics used were:

**Mel-Cepstral Distortion (MCD)** [55]: MCD quantifies the spectral distance between the mel-frequency cepstral coefficients (MFCCs).

**Gross Pitch Error (GPE)** [56]: GPE measures the proportion of voiced frames where the estimated fundamental frequency (pitch) deviates by more than 20% from  $s * r$ , primarily assessing prosodic information preservation.

**Speaker Similarity (SPK-sim):** SPK-sim evaluates the preservation of speaker identity. We computed a cosine similarity of the speaker embedding [57], [58] extracted from the ground truth reverberant speech and the model.

The objective evaluation results, including scores for noisy input and Miipher-2 [26] which predicts  $s$ , are presented in Table 2. ReverbMiipher achieves the best performance among the three compared models across all three metrics, indicating its success in preserving the reverberance of the input speech. ReverbMiipher outperforms Miipher-RIR. Thus, we observe better performance when stochastically integrating the encoding of reverberation within the SR model, as opposed to adding reverberation to clean speech in a post-hoc manner. The GPE results also suggest that the Miipher-RIR baseline degrades the prosodic information of the original speech. Fig. 2 shows an example of restoration result using ReverbMiipher. Although the noisy input contains reverberation as well as noise and the effects of a low-pass filter, we can see that ReverbMiipher removes all signal degradation except for reverberation.

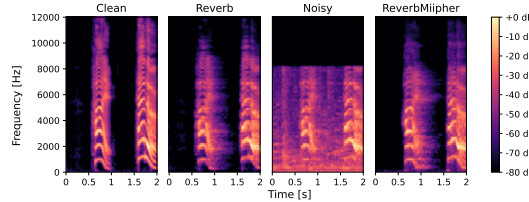


Fig. 2: SR result with ReverbMiipher. From the left, the spectrograms of clean signal  $s$ , reverberant target  $s * r$ , noisy input  $x$ , and output  $y$ , respectively.

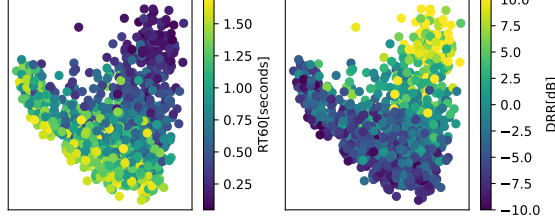


Fig. 3: PCA-based latent space distribution of reverb feature with respect to RT60 (left) and DRR (right).

## 5. ANALYSIS AND APPLICATIONS

### 5.1. Visualization of reverb-feature distribution

We investigated the relationship between our proposed reverberation feature,  $c$ , and standard reverberation metrics (RT60 and DRR) using PCA visualization. Test signals were created by convolving speech from the EARS corpus with synthetic RIRs generated via pyroomacoustics [46]. For each signal, we extracted  $c$  and calculated the RT60 (Schroeder method [59]) and DRR from RIRs.

Fig. 3 displays the PCA projection, mapping  $c$  against RT60 and DRR. Results show  $c$  changes continuously relative to both standard metrics. This smooth variation supports the use of  $c$  for implementing fine-grained, continuous user control over reverberance during speech restoration. Furthermore, the visualization shows anechoic samples clustering in the upper right, while increasing reverberation causes the data points to spread towards the upper left and lower right. This dispersion highlights the feature's ability to capture the widening range of acoustic properties characteristic of more reverberant environments.

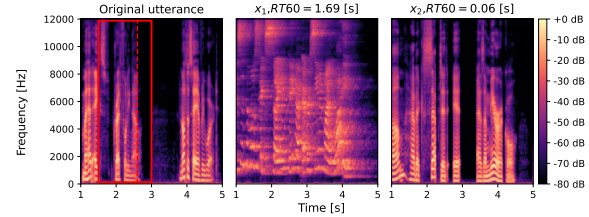
### 5.2. Reverb-feature interpolation

Given the observed continuity of the reverb feature concerning reverberation parameters such as RT60 and DRR (Fig. 3), linear interpolation presents a viable method for generating novel reverberant effects. Let  $c_1$  and  $c_2$  be a reverb features extracted from utterances  $x_1$  and  $x_2$ . Interpolated reverb feature,  $c(\alpha)$ , can be computed from  $c_1$  and  $c_2$ , using a weight  $\alpha$  as  $c(\alpha) = (1 - \alpha)c_1 + \alpha c_2$ , for  $0 \leq \alpha \leq 1$ .

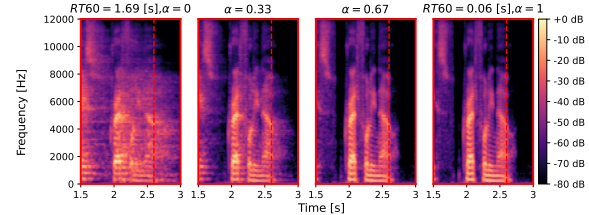
Fig. 4b illustrates the result of applying interpolated reverb features to speech synthesis, visualized via mel spectrograms. For this demonstration,  $c_1$  corresponds to a highly reverberant condition (RT60 = 1.69 s) and  $c_2$  to a near-anechoic condition (RT60 = 0.06 s) as shown in Fig. 4a. The result confirms that varying  $\alpha$  from 0 to 1 yields continuous modification of reverberance, while maintaining its harmonic structure integrity. This shows that it is possible to control the perceived reverberation through straightforward linear manipulation of the proposed feature. Corresponding audio samples can be found online<sup>1</sup>.

### 5.3. Reverb-feature sampling

The reverberation interpolation method in ReverbMiipher assumes the user provides reference speech with reverberation characteristics



(a) Original utterance,  $x_1$  and  $x_2$  used for reverb feature interpolation.  $x_1$  corresponds to reverberant speech (RT60 = 1.69 seconds) and  $x_2$  corresponds to the non-reverberant speech (RT60 = 0.06 seconds). Red box corresponds to the zoomed-in section in Fig. 4b



(b) Zoomed-in visualization of reverb feature interpolation. Red dashed line shows the part where the reverberation change is clearly visible.

Fig. 4: Reverb feature interpolation inputs and corresponding output with different  $\alpha$ .

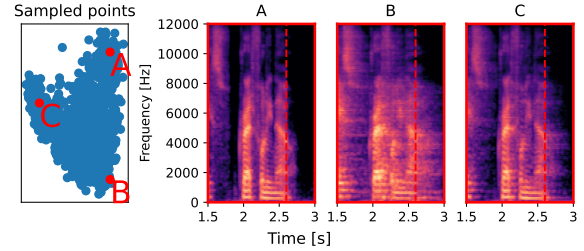


Fig. 5: Reverb feature sampling from PCA-based latent space. The original utterance is the same as the Fig. 4a

similar to the desired output, which limits its applicability. Therefore, we also explored an alternative approach where the reverberation feature is sampled directly from its latent space. Specifically, we sampled features from the two-dimensional plane derived from the aforementioned PCA analysis. Fig. 5 presents the results of this sampling strategy. The results demonstrate that the original speech structure is preserved while the level of reverberance changes for each sampled feature. This suggests that the straightforward strategy of sampling from the human understandable 2D PCA plane is viable for controlling reverberation. Audio samples can be found online<sup>1</sup>.

## 6. CONCLUSION

In this paper, we introduced ReverbMiipher: an SR model designed to preserve and manipulate reverberation while removing unwanted distortions such as additive noise or codec artifacts. ReverbMiipher extends the Miipher-2 SR model with a reverb encoder that extracts reverberation-related features from the noisy speech input. Experimental results show that ReverbMiipher preserves reverberation better than to the baseline approach, which uses ground truth RIR reverberation characteristics for preservation. We also demonstrated that the reverberation manipulation is possible with both reverberation interpolation and reverb feature sampling. Future work includes preservation or manipulation of other acoustically-encoded information, such as environmental sounds, for SR.

## REFERENCES

[1] H. Kuttruff, *Room Acoustics*. Wiley, 1973.

[2] W. Bailey and B. M. Fazenda, “The effect of reverberation and audio spatialization on egocentric distance estimation of objects in stereoscopic virtual reality,” *J. Acoust. Soc. Am.*, 2017.

[3] D. R. Begault, E. M. Wenzel, and M. R. Anderson, “Direct comparison of the impact of head tracking, reverberation, and individualized head-related transfer functions on the spatial perception of a virtual speech source,” *J. AES*, 2001.

[4] P. Larsson, A. Välijämäe, *et al.*, “Auditory-induced presence in mixed reality environments and related technology,” *The engineering of mixed reality systems*, 2010.

[5] R. Rombach, A. Blattmann, *et al.*, “High-resolution image synthesis with latent diffusion models,” in *CVPR*, 2022.

[6] Z. Borsos, R. Marinier, *et al.*, “AudioLM: a language modeling approach to audio generation,” *IEEE/ACM Trans. Audio, Speech and Lang. Proc.*, 2023.

[7] P. A. Naylor and N. D. Gaubitch, *Speech Dereverberation*. Springer, 2010.

[8] T. Nakatani, T. Yoshioka, *et al.*, “Speech dereverberation based on variance-normalized delayed linear prediction,” *IEEE/ACM Trans. Audio, Speech and Lang. Proc.*, 2010.

[9] K. Kinoshita, M. Delcroix, *et al.*, “The REVERB challenge: A common evaluation framework for dereverberation and recognition of reverberant speech,” in *WASPAA*, 2013.

[10] K. Han, Y. Wang, and D. Wang, “Learning spectral mapping for speech dereverberation,” in *ICASSP*, 2014.

[11] K. Kinoshita, M. Delcroix, *et al.*, “Neural network-based spectrum estimation for online wpe dereverberation.” in *Interspeech*, 2017.

[12] N. Das, S. Chakraborty, *et al.*, “Fundamentals, present and future perspectives of speech enhancement,” *Int. J. of Speech Tech.*, 2021.

[13] S. Maiti and M. I. Mandel, “Parametric resynthesis with neural vocoders,” in *WASPAA*, 2019.

[14] T. Saeki, S. Takamichi, *et al.*, “SelfRemaster: Self-supervised speech restoration with analysis-by-synthesis approach using channel modeling,” in *Interspeech*, 2022.

[15] J. Su, Z. Jin, and A. Finkelstein, “HiFi-GAN-2: Studio-quality speech enhancement via generative adversarial networks conditioned on acoustic features,” in *WASPAA*, 2021.

[16] H. Liu, X. Liu, *et al.*, “VoiceFixer: A unified framework for high-fidelity speech restoration,” in *Interspeech*, 2022.

[17] J. Serrà, S. Pascual, *et al.*, “Universal speech enhancement with score-based diffusion,” *arXiv preprint arXiv:2206.03065*, 2022.

[18] Y. Koizumi, H. Zen, *et al.*, “Miipher: A robust speech restoration model integrating self-supervised speech and text representations,” in *WASPAA*, 2023.

[19] J. Richter, S. Welker, *et al.*, “Speech enhancement and dereverberation with diffusion-based generative models,” *IEEE/ACM Trans. Audio, Speech and Lang. Proc.*, 2023.

[20] J.-M. Lemercier, J. Richter, *et al.*, “Diffusion models for audio restoration: A review,” *IEEE Signal Process Mag.*, 2024.

[21] R. Scheibler, Y. Fujita, *et al.*, “Universal score-based speech enhancement with high content preservation,” in *Interspeech*, 2024.

[22] B. Kang, X. Zhu, *et al.*, “LLaSE-G1: Incentivizing generalization capability for llama-based speech enhancement,” *arXiv preprint arXiv:2503.00493*, 2025.

[23] H. Yang, J. Su, *et al.*, “Genhancer: High-fidelity speech enhancement via generative modeling on discrete codec tokens,” in *Interspeech*, 2024.

[24] X. Liu, X. Li, *et al.*, “Joint semantic knowledge distillation and masked acoustic modeling for full-band speech restoration with improved intelligibility,” in *ICASSP*, 2025.

[25] H. R. Guimarães, J. Su, *et al.*, “DiTSE: High-fidelity generative speech enhancement via latent diffusion transformers,” *arXiv preprint arXiv:2504.09381*, 2025.

[26] S. Karita, Y. Koizumi, *et al.*, “Miipher-2: A universal speech restoration model for million-hour scale data restoration,” *arXiv preprint arXiv:2505.04457*, 2025.

[27] A. Gupta, L. Yu, *et al.*, “Photorealistic video generation with diffusion models,” in *ECCV*, 2023.

[28] A. Blattmann, T. Dockhorn, *et al.*, “Stable video diffusion: Scaling latent video diffusion models to large datasets,” *arXiv preprint arXiv:2311.15127*, 2023.

[29] J. B. Allen and D. A. Berkley, “Image method for efficiently simulating small-room acoustics,” *J. Acoust. Soc. Am.*, 1979.

[30] Z. Xu, A. Herzog, *et al.*, “Simulating room transfer functions between transducers mounted on audio devices using a modified image source method,” *The J. of the Acoust. Soc. Am.*, 2024.

[31] B. Hamilton and S. Bilbao, “FDTD methods for 3-d room acoustics simulation with high-order accuracy in space and time,” *IEEE/ACM Trans. Audio, Speech and Lang. Proc.*, 2017.

[32] A. Luo, Y. Du, *et al.*, “Learning neural acoustic fields,” in *NeurIPS*, 2022.

[33] A. Ratnarajah, Z. Tang, and D. Manocha, “IR-GAN: Room Impulse Response Generator for Far-Field Speech Recognition,” in *Interspeech*, 2021.

[34] C. J. Steinmetz, V. K. Ithapu, and P. Calamia, “Filtered noise shaping for time domain room impulse response estimation from reverberant speech,” in *WASPAA*, 2021.

[35] Y. Choi, C. Xie, and T. Toda, “Reverberation-controllable voice conversion using reverberation time estimator,” in *Interspeech*, 2023.

[36] S. He and R. Liu, “Multi-source spatial knowledge understanding for immersive visual text-to-speech,” in *ICASSP*, 2025.

[37] D. Wang and J. Chen, “Supervised speech separation based on deep learning: An overview,” *IEEE/ACM Trans. Audio, Speech and Lang. Proc.*, 2018.

[38] P. Záviška, P. Rajmic, *et al.*, “A survey and an extensive evaluation of popular audio declipping methods,” *IEEE Journal of Selected Topics in Signal Processing*, 2020.

[39] K. Li and C.-H. Lee, “A deep neural network approach to speech bandwidth expansion,” in *ICASSP*, 2015.

[40] V. Kuleshov, S. Z. Enam, and S. Ermon, “Audio super-resolution using neural nets,” in *ICLR (Workshop Track)*, 2017.

[41] W. Zhang, R. Scheibler, *et al.*, “Neurips 2024 competition proposal: Urgent challenge,” in *NeurIPS 2024 Competition Track*.

[42] Y. Zhang, W. Han, *et al.*, “Google USM: Scaling automatic speech recognition beyond 100 languages,” 2023.

[43] J. He, C. Zhou, *et al.*, “Towards a unified view of parameter-efficient transfer learning,” in *ICLR*, 2022.

[44] A. Gulati, C.-C. Chiu, *et al.*, “Conformer: Convolution-augmented transformer for speech recognition,” in *Interspeech*, 2020.

[45] Y. Koizumi, K. Yatabe, *et al.*, “WaveFit: An iterative and non-autoregressive neural vocoder based on fixed-point iteration,” in *SLT*, 2023.

[46] R. Scheibler, E. Bezzam, and I. Dokmanić, “Pyroomacoustics: A python package for audio room simulation and array processing algorithms,” in *ICASSP*, 2018.

[47] W. Mack, S. Deng, and E. A. Habets, “Single-channel blind direct-to-reverberation ratio estimation using masking,” in *Interspeech*, 2020.

[48] M. Ma, Y. Koizumi, *et al.*, “FLEURS-R: A restored multilingual speech corpus for generation tasks,” in *Interspeech*, 2024.

[49] J. Richter, Y.-C. Wu, *et al.*, “EARS: An anechoic fullband speech dataset benchmarked for speech enhancement and dereverberation,” in *Interspeech*, 2024.

[50] G. Wichern, J. Antognini, *et al.*, “WHAM!: Extending speech separation to noisy environments,” in *Interspeech*, 2019.

[51] J. Traer and J. H. McDermott, “Statistics of natural reverberation enable perceptual separation of sound and space,” *Proceedings of the National Academy of Sciences*, 2016.

[52] D. P. Kingma and J. Ba, “Adam: A method for stochastic optimization.” in *ICLR*, 2015.

[53] W. J. Conover, *Practical nonparametric statistics*. John Wiley & Sons, 1999.

[54] O. J. Dunn, “Multiple comparisons among means,” *Journal of the American Statistical Association*, 1961.

[55] R. Kubichek, “Mel-cepstral distance measure for objective speech quality assessment,” in *PACRIM*, 1993.

[56] W. Chu and A. Alwan, “Reducing f0 frame error of f0 tracking algorithms under noisy conditions with an unvoiced/voiced classification frontend,” in *ICASSP*, 2009.

[57] Y. Jia, Y. Zhang, *et al.*, “Transfer learning from speaker verification to multispeaker text-to-speech synthesis,” in *NeurIPS*, 2018.

[58] Y. Chen, Y. Assael, *et al.*, “Sample efficient adaptive text-to-speech,” in *ICLR*, 2019.

[59] M. R. Schroeder, “New method of measuring reverberation time,” *The Journal of the Acoustical Society of America*, 1965.